Knockdown Of Udp-Glucose Dehydrogenase Facilitates Epirubicin-Resistance In MDA-MB-231 Breast Cancer Cells By Regulation Of Hyaluronan Synthesis.

Daiana L. Vitale
Universidad Nacional del Noroeste de la Provincia de Buenos Aires
Ilaria Caon
Universita degli Studi dell'Insubria
Arianna Parnigoni
Universita degli Studi dell'Insubria
Ina Sevic
Universidad Nacional del Noroeste de la Provincia de Buenos Aires
Fiorella M. Spinelli
Universidad Nacional del Noroeste de la Provincia de Buenos Aires
Antonella Icardi
Universidad Nacional del Noroeste de la Provincia de Buenos Aires
Alberto Passi
Universita degli Studi dell'Insubria
Davide Vigetti
Universita degli Studi dell'Insubria
Laura Daniela Alaniz (ldalaniz@comunidad.unnoba.edu.ar)
Universidad Nacional del Noroeste de la Provincia de Buenos Aires https://orcid.org/0000-0002-6070-6078

Research

Keywords: MDA-MB-231, Breast Cancer

Posted Date: September 1st, 2020

DOI: https://doi.org/10.21203/rs.3.rs-66926/v1

Abstract

Background: The catalytic action of the UDP-glucose transferase dehydrogenase (UGDH) enzyme produces UDP-glucuronic acid (UDP-GlcUA). The main detoxifying pathway of Epirubicin (EPI) is via glucuronidation by the specific transferase UGT2B7 (UDP-Glucuronosyltransferase-2B7), adding UDP-GlcUA to generates 4´-O-b-D-glucuronyl-4´-epi-doxorubicin. UDP-GlcUA is also a precursor of several glycosaminoglycans (GAGs) like hyaluronan (HA). Therefore, the EPI detoxifying pathway might be associated with GAGs metabolism, related to drug deactivation and tumor resistance. This work aimed to evaluate the effect of knockdown on the UGDH gene on EPI response and HA metabolism in the aggressive breast cancer cells MDA-MB 231.

Methods: MDA-MB-231 cells were transfected *in vitro* with UGDH-specific siRNA for UGDH knockdown and treated with EPI. Viability, apoptosis, and cytotoxicity effects were evaluated. EPI intracellular accumulation was analyzed by flow cytometry. Differences in extracellular matrix (ECM) were analyzed through a particle exclusion assay and the composition of HA using hyaluronidase. The soluble HA secreted was detected by an ELISA like assay. Besides, gene expression of HA synthase and hyaluronidase (HYAL) enzymes were analyzed by RT-qPCR. To analyze the effect of UGDH knockdown and EPI treatment on autophagy, we evaluated the expression of the autophagosome marker, LC3-II by RT-qPCR and western blot, and its subcellular localization by confocal microscopy.

Results: EPI accumulation increased during UGDH knockdown, but it was observed a decrease in cell death. HA synthesis and HA coated around the cells increased. In turn, it was found up-regulation of the expression of HYALs. Within the mechanisms activated by tumor cells to avoid EPI activity, an increase in autophagy was detected.

Conclusions: for the first time we show that an increase in the expression, deposition and catabolism of HA positively contributed to the development of a resistant phenotype in breast cancer cells by a mechanism associated to sugar metabolism, specifically of UDP-GlcUA .

Introduction

Anthracyclines rank among the most effective antitumor drugs ever developed. The first molecules established within this family were doxorubicin (DOX) and daunomycin, and beyond being effective, both drugs soon proved to be hampered by serious problems like the development of resistance in tumor cells or toxicity in healthy tissues [1].

In the last decades, there were numerous attempts to identify novel anthracyclines that proved superior in terms of activity and cardiac tolerability. Few analogs have reached the stage of clinical development and the FDA approval; among them, epirubicin (EPI) and idarubicin are useful alternatives to other anthracyclines. Despite extensive clinical use, the mechanisms of resistance emerged during the treatment. In the last decades, EPI has been widely used for the treatment of metastatic diseases as adjuvant therapy and is one of the most active drugs employed in the chemotherapy treatment of

patients with breast cancer after surgery and in progression in arm lymph nodes. Furthermore, anthracyclines, like EPI are widely used in the treatment of hormone-resistant breast cancer. These types of tumors are considered triple-negative due to the lack of expression of three specific markers: the progesterone receptor, the estrogen receptor and HER2 protein. Due to that deficiency, triple-negative tumors do not respond to hormonal treatment, consequently, patients are referred to anthracycline treatment [2, 3]. EPI is a semisynthetic derivative of DOX, which has similar efficacy but less adverse effects at equimolar doses. It is obtained by an axial-to-equatorial epimerization of the hydroxyl group at C-4 in daunosamine [4]. This positional change has a slight effect on the mechanism of action and the spectrum of activity of EPI compared with DOX. However, it introduces pharmacokinetic and metabolic changes like increased volume of distribution, elimination through 4-*O*-glucuronidation, and consequent enhanced total body clearance, or shorter terminal half-life [5, 6].

EPI is extensively metabolized in the liver, like other anthracyclines. The main detoxifying pathway is the formation of a glucuronide form of EPI (4´-*O*-b-D-glucuronyl-4´-epi-doxorubicin) via a glucuronidation reaction. It has an important role in drug detoxification and clearance and represents a protective mechanism to improved eliminate of lipophilic xenobiotics from the organism [7]. Glucuronidation is carried out by UDP-glucuronosyltransferases enzymes (UGTs), classified into subfamilies based on their amino acid sequence homology [8]. EPI is mainly glucuronidated by the addition of one molecule of UDP-glucuronic acid (UDP-GlcUA), through the action of the specific UGT called UGT2B7 [9].

The development of drug resistance limits the efficacy of anthracyclines and other antineoplastic therapies [10]. In particular, the development of resistance to EPI can occur via different mechanisms, including P-glycoprotein-mediated resistance, changes in topoisomerase II activity, induction of heat shock proteins and inhibition of apoptotic pathways [11]. On the other hand, since EPI is glucuronidated by UGT2B7, factors that modulate UGT2B7 expression and activity would have a potential impact on EPI systemic clearance and efficacy. Indeed, it has been demonstrated that EPI upregulates UGT2B7 expression in hepatocellular carcinoma HepG2 and Huh7 cells via p53 [12], suggesting that detoxifying genes are activated by the p53-mediated pathway to clear genotoxic agents locally within the tumor site or even systemically through the liver. It has also been observed that cell autophagy protects MCF-7 breast cancer cells from EPI-induced apoptosis and facilitates EPI resistance development acting as a pro-survival factor [13].

In addition to taking part in EPI glucuronidation, UDP-GlcUA is a precursor of several glycosaminoglycans (GAGs) and proteoglycans (PGs) present in the extracellular matrix (ECM). UDP-GlcUA is formed by the oxidation of UDP-glucose through the catalytic action of the UDP-glucose dehydrogenase (UGDH) enzyme [14]. Once UDP-GlcUA is formed, it can be a substrate of different divergent pathways [15]. Thus, the UGDH is involved in the modification of hormones or xenobiotics, such as EPI, for their solubilization and elimination [16]. Moreover, it is involved in hyaluronan (HA) synthesis, through the catalytic action of HA synthases (HAS1, HAS2 and HAS3) [17], as well as in the polymerization of heparan sulfate chains. Lastly, due to the conversion to UDP-xylose, it initiates the production of different proteoglycans, such as chondroitin sulfate [18].

In cancer development it is well known that HA expression is usually altered, affecting several mechanisms associated, among others, with cell proliferation and survival, invasion, angiogenesis and multidrug resistance, [19–24]. Even more, it has been recently demonstrated that HA also affects immune cells recruitment and inflammation [25]. On the other hand, UGDH has been proposed as a novel candidate biomarker of prostate cancer that may complement the development of a multi-biomarker panel for detecting tumor transformation within the adjacent tumor tissue [26]. Even more, it has been determined that the treatment of colorectal carcinoma HCT-8 cells with either UGDH-specific small interference RNA (siRNA) or HA synthesis inhibitor 4-methylumbelliferone (4-MU), effectively delayed cell aggregation and impaired cell motility. These results propose UGDH as a potential target for therapeutic intervention of colorectal cancers. The importance of glucuronidation reaction and the role of the UGDH enzyme in breast cancer treatment has not yet been studied.

Furthermore, a possible modulation of these mechanisms by EPI in tumor microenvironment would be clinically relevant. Therefore, this work aimed to evaluate the effect of silencing the UGDH gene with a specific siRNA on EPI response using an aggressive breast cancer cell line. Even more, tumor cells responded to both conditions increasing its ECM as another mechanism of tumor drug resistance.

Materials And Methods

Reagents

Amaxa® Cell Line Nucleofector® Kit V was purchased from Lonza Cologne AG (Germany). High glucose Dulbecco's modified Eagle's medium (DMEM) was from EuroClone S.p.A. (Italy). EPI was purchased from Selleckchem (USA). Anti-β-catenin antibody was purchased from Millipore (USA). A specific antibody against glyceraldehyde-3-phosphate dehydrogenase (GAPDH) was taken from NeoBioLab (USA). Anti-phosphorylated Akt (Ser473, Ser472 and Ser474) antibody was purchased from R&D System (USA) and anti-rabbit secondary horseradish peroxidase (HRP) antibody was purchased from Santa Cruz Biotechnology (USA). Annexin V-FITC apoptosis detection kit was from BioVision (USA). LDH-cytotoxicity Assay Kit was purchased from Abcam (UK).

Cell culture

The immortalized human breast adenocarcinoma cell line MDA-MB-231 (ATCC® HTB-26) was maintained in exponential growth by serial passages in DMEM-high glucose medium supplemented with 2 mM L-glutamine, 100 IU penicillin, 100 µg/ml streptomycin and 10% v/v of fetal bovine serum (FBS) in a humidified incubator at 37 °C and 5% CO_2. During all cell cultures, periodic checkups of cell morphology and growth rate were performed, as well as the strict control of cell line passages (5-10th passage). MDA-MB-231 cell line was authenticated by Northgene Ltd. Company (UK), using highly sensitive DNA testing for Short Tandem Repeats (STR). The cell line was also analyzed to discard the presence of mycoplasma contamination by PCR [27].

Transfection and EPI treatment

MDA-MB-231 cells were plated in a 6 well-plate (1×10^6) and transfected through nucleoporation with 30 nM of UGDH small interference RNA (siRNA, siUGDH) or a negative control siRNA (siSCR) having a random sequence, using the Amaxa® Cell Line Nucleofector® Kit V. After 24 h of incubation, 1 μM of EPI (EPI) was added to complete 48 h of incubation after transfection in combination with both siRNAs (siUGDH + EPI and siSCR + EPI). EPI treatment was performed to compare the results caused by the drug, as well as a control without transfection (Basal). During both treatments, cells were maintained in a humidified incubator at 37 °C and 5% CO_2. Subsequently, supernatants were collected and conserved at -80ºC until their use.

Viability assay

After the transfection with siRNA UGDH and EPI treatment, MDA-MB-231 cells (1×10^3) were plated in a 96-well plate and incubated at 37 °C and 5% CO_2 for 24 h. All samples were treated with 50 ul per well of 3-(4,5-Dimethyl-2-thiazolyl)-2,5-diphenyl-2H-tetrazolium·bromide (Serva) and incubated at 37 °C for 4 h. After adding 200 μl/well of DMSO to dissolve crystals, optical density (OD) was quantified by spectrophotometer at 570 nm.

Cytotoxicity assay

Cellular cytotoxicity was evaluated through the measurement of the activity of lactate dehydrogenase (LDH) enzyme released from damaged cells using the specific LDH Cytotoxicity Assay Kit (Abcam). LDH enzyme oxidizes lactate to pyruvate, which reacts with a tetrazolium salt (INT) to form formazan. Supernatants of transfected and treated cells were analyzed following the manufacturer's protocol.

Epirubicin accumulation assay

EPI is a single molecule capable of emitting fluorescence detectable by flow cytometry (550–600 nm). EPI intracellular accumulation was analyzed as we previously described [27]. MDA-MB-231 cells (5×10^5) were transfected and treated as mentioned above and EPI fluorescence was collected through a 564–606 nm band-pass filter. Samples were analyzed using a FACS Aria II cytometer and data was evaluated using FlowJo 5 software (Becton, Dickinson and Company, USA).

Apoptosis detection assay

To evaluate apoptosis, the MDA-MB-231 cells (5×10^5) were transfected and treated as mentioned above. After culture procedures, cells were stained with annexin V-FITC reagent for 30 minutes at room temperature following the manufacturer´s protocol. Samples were analyzed using FACS Aria II cytometer and data were evaluated using FlowJo 5 software (Becton, Dickinson and Company, USA).

RT-qPCR

Total RNA from MDA-MB-231 cells (1×10^6) was extracted using PureLink® RNA Mini Kit Life Technologies (Life Technologies). RNA integrity and quantification were assessed by spectrophotometry system, measuring OD260 and OD280 in Nanodrop® instrument. Two micrograms of RNA were reverse transcribed using High Capacity cDNA Reverse Transcription Kit (Applied Biosystems).

cDNAs were analyzed by quantitative real time PCR (RT-qPCR) using FastStart SYBR Green: UGT2B7 (Fw: 5´ GGA GAA TTT CAT CAT GCA ACA GA 3´ and Rv: 5´ CAG AAC TTT CTA GTT ATG TCA CCA AAT ATT G 3´); ABCC1 (Fw: 5´ AAG TCG GGG CAT ATT CCT G 3´ and Rv: 5´ TGA AGA CTG AAC TCC CTT CCT C 3´); ABCC2 (Fw: 5´ AAA TCC AGG ACC AAG AGA TCC 3´ and Rv: 5´ TGT GGC TTG TCC AGA GTC TTC 3´); ABCG2 (Fw: 5´ GCT GCA AGG AAA GAT CCA AG 3´ and Rv: 5´ CAG AGT GCC CAT CAC AAC ATC 3´); VEGF (Fw: 5´ CTA CCT CCA CCA TGC CAA GT 3´ and Rv: 5´ GCA GTA GCT GCG CTG ATA GA 3´); EGF (Fw: 5´ TGA TAA GCG GCT GTT TTG G 3´ and Rv: 5´ CAC CAA AAA GGG ACA TTG C 3´); HYAL-1 (Fw: 5´ GGC TAT GAG GAA ACT GAG TCA C 3´ and Rv: 5´ TAG GAG TGC AAG GGC TGT AC 3´); HYAL-2 (Fw: 5´ ATC TCT ACC ATT GGC GAG AGT G 3´ and Rv: 5´ ATC TTT GAG GTA CTG GCA GGT C 3´); HYAL-3 (Fw: 5´ TAT GTC CGC CTC ACA CAC C 3´ and Rv: 5´ CTG CAC TCA CAC CAA TGG AC 3´) and LC3-II (Fw: 5´ AGC AGC ATC CAA CCA AAA TC 3´ and Rv: 5´ CTG TGT CCG TTC ACC AAC AG 3´) or Taqman® probes: UGDH (Hs00163365_m1), HAS2, (Hs00193435_m1) and HAS3 (Hs00193436_m1) assays (Applied Biosystems).

PCR conditions for SYBR Green reactions were 90 seconds at 94 °C and then 40 cycles of 30 seconds at 94 °C, 30 seconds at 60 °C and 30 seconds at 72 °C. PCR conditions for probes reactions were 2 minutes at 50 °C, 10 minutes at 95 °C and then 40 cycles of 15 seconds at 95 °C and 60 seconds at 60 °C. All the assays were performed using Abi 7000 Sequence Detection System instrument (Applied Biosystems). Results were normalized using β-actin (Fw: 5´ GGG GCT GCC CAG AAC ATC AT 3´ and Rv: 5´ GCC TGC TTC ACC ACC TTC TTG 3´), as a reference gene and all determinations were performed as duplicates in three separated experiments. A non-template control (NTC) was correspondingly added during every assay.

Protein extracts and western blot

To analyze protein expression, MDA-MB-231 cells (1×10^6) were transfected and treated with EPI as described above and then were lysed with RIPA lysis buffer ON at 4 °C [28]. After centrifugation, supernatants were preserved, and protein concentration was measured using Bradford protein assay. Protein extracts were stored at -80 °C until its use. Equal amounts of protein were resolved by 0.1% SDS-10% polyacrylamide gel denaturing electrophoresis (SDS-PAGE) and transferred onto a nitrocellulose membrane. For LC3 proteins, we used a tricine SDS-PAGE with 16% polyacrylamide 6M urea gel [29]. The membranes were incubated with a specific anti-β-catenin, anti-p-Akt, anti-LC3-I, anti-LC3-II and anti-GAPDH antibodies ON at 4 °C, and then incubated with horseradish peroxidase-labeled secondary antibody for 1.5 hours at RT. Finally, HRP chemiluminescence reaction was detected using a stable peroxide solution and an enhanced luminol solution. Images were obtained with an ImageQuant 4000 mini bioluminescent image analyzer (GE HealthCare LifeSciences) and analyzed using ImageJ 1.50b software package (National Institutes of Health, USA).

Wound healing assay

MDA-MB-231 migration ability after transfection and EPI treatment was analyzed performing a wound healing assay. MDA-MB-231 cells (1×10^6) were transfected as mentioned above. After EPI treatment, consistently shaped wounds were made using a sterile 100 µl pipette tip across each well, creating a cell-free area line [30]. Three images were captured in the same coordinates point at 0, 4, 8 and 22 h after

performing the wound. The gap size of the wounds was measured and analyzed using ImageJ 1.50b software package (National Institutes of Health, USA). The results obtained were expressed considering the decrease in the initial area of the wound, considered as 100% at time 0.

VEGF and FGF-2 ELISA

Secreted levels of Human VEGF were determined by DuoSet ELISA Kit (R&D System, USA) from free-cell culture supernatants collected after treatments. FGF-2 expression levels were determined by DuoSet ELISA Kit (R&D System, USA) from protein extracts. The assays were carried out according to instructions provided by the manufacturer.

Particle exclusion assay

Variations in ECM after siUGDH transfection and EPI treatment were analyzed through a particle exclusion assay [31]. MDA-MB-231 cells were plated in a 12 well-plate (3×10^4) and transfected with UGDH siRNA or negative control siRNA, as described above. After 24 h, 1 μM EPI was added to complete 48 h of incubation after transfection. To determine the proportion of the pericellular area composed of HA, specific controls with active and heated inactivated-hyaluronidase from S. *hyaluroliticus* (SIGMA) were also performed during the assay, treating the tumor cells with two U/ml of hyaluronidase for 1 hour. When treatments were completed, MDA-MB-231 cells were washed with PBS and 2×10^7 fixed red blood cells were added to each well. After allowing red blood cells to decant for 30 minutes in an incubator, images of each condition were capture and analyzed using ImageJ 1.50b software package (National Institutes of Health, USA).

ELISA-like assay for detection of soluble HA

Since the HA synthesized can be secreted or can remain anchored to the cell membrane, it was decided to evaluate the concentration of this GAG in cell supernatants. The protocol used was adapted from previous studies [32] and developed by our laboratory. A “sandwich” strategy was followed in which a specific HA-binding protein (HABP) was used to cover a 96-well plate. Once the samples of cell supernatants from the MDA-MB-231 cells were placed, HABP protein was added in its biotinylated form to determine the concentration of HA through the colorimetric detection of the peroxidase enzyme activity.

Confocal microscopy for LC3 subcellular localization

MDA-MB-231 cells were plated on coverslips and co-transfected with UGDH or negative control siRNA plus two μg of EGFP-LC3 (# 11546, Addgene). 24 h after transfection, tumor cells were treated with1 μM EPI as described above. After the treatment, the medium was removed, and cells were mounted on glass slides after being washed twice in PBS and fixed in 4% formaldehyde for 30 min. LC3 subcellular localization was analyzed by confocal microscopy using a Leica TCS SP5 instrument. The experiment was also performed treating each well with 20 μM chloroquine (an inhibitor of autophagy). Chloroquine was added to the cells concomitantly with EPI.

LDH activity assay

To determine the activity of intracellular LDH enzyme, MDA-MB-231 cells were transfected and treated with EPI as described above. LDH activity was analyzed in cell lysates using the specific kit LDH Cytotoxicity Assay Kit (Abcam) following the manufacturer's protocol.

Statistical analysis

For statistical analysis, 95% confidence intervals (CI) were determined by calculating arithmetic mean values and variance (standard error of the mean, SEM) of three independent experiments. To evaluate if differences between the obtained values were significant: T Student's test (T-test, Mann-Whitney) was used in the case of comparisons between two groups, or analysis of variance (ANOVA, Tukey Test) was also used to evaluate the differences between values of more than two experimental groups. The software Prism (GraphPad 5, San Diego, CA, USA) was used, considering a p value < 0.05 as statistically significant.

Results

Analysis of UGDH expression and cell integrity after UGDH knockdown and EPI treatment

First, to verify that our transfection system worked correctly, it was decided to analyze the expression levels of UGDH after completing the transfection scheme and post-treatment with EPI. As expected, after 48 hours, MDA-MB-231 cells transfected with UGDH-specific siRNA showed a significant reduction in UGDH expression levels (siUGDH, 90% respect to control). Surprisingly, we found a significant increase in the expression of UGDH in response to the treatment with 1 μM EPI (EPI) *(***$p < 0.001$)*. However, the silencing of UGDH combined with EPI treatment (siUGDH + EPI) produced a significant reduction of UGDH mRNA levels respect to EPI (Fig. 1A).

An important consideration during transfection experiments is to monitor possible alterations in cell integrity during cell culture because of nucleofection and antitumor treatment with EPI. For that reason, we decided to evaluate the effect of both transfection and EPI treatment on cell viability, cytotoxicity, and apoptosis.

As expected, only the treatment with EPI decreased cell viability in a 40%, since we used a concentration close to IC50 value ($IC50_{MDA-MB-231}$: 4.9 μM) in order to obtain viable cells for subsequent assays (*$p < 0.05$), as was determined previously [27]. A decrease in cell viability was found when comparing transfections with siUGDH siSCR (data not shown), which could be related to the transfection method. Although a slight accentuation of this effect was observed in the presence of EPI (siUGDH + EPI and siSCR + EPI respectively), these differences were not statistically significant, and the levels remained above the values of treatment with 1 EPI (Fig. 1B). Cell viability of siSCR control did not differ significantly from the basal control (data not shown).

When cytotoxicity was evaluated by realizing of LDH enzyme, we observed increased levels in all conditions in which cells were transfected (Fig. 1C). This result was expected since the transfection method involves the electroporation of the cell membrane that can release this enzyme to the culture

medium and not allowed us to observe differences with EPI treatment. Finally, we found unexpected results analyzing the induction of apoptosis after transfection and EPI treatment. We observed higher levels of apoptosis after EPI treatment compared to basal conditions (EPI vs. BASAL **p < 0.01*). However, apoptosis induction after silencing of UGDH and EPI treatment was significantly reduced compared with transfected cells without EPI treatment (siUGDH + EPI vs. siUGDH **p < 0.05*). Nevertheless, apoptosis levels in those conditions (siUGDH + EPI) remained below the levels obtained with 1 μM EPI treatment (EPI) (Fig. 1D and 1E). Therefore, the knockdown of UGDH during EPI treatment affected apoptosis induction in MDA-MB 231 tumor cells.

Evaluation of intracellular accumulation of EPI after knockdown of UGDH enzyme

EPI is a molecule capable of emitting fluorescence in the red spectrum, which is detectable in flow cytometry assays (excitation peak 480 nm and emission peak 590 nm). This allowed the intracellular analysis of EPI accumulation in MDA-MB-231 cells after transfection of siUGDH or siSCR, evidencing the appearance of positive fluorescence in this spectrum.

We observed a higher EPI intracellular accumulation in tumor cells that had been transfected with siUGDH compared with no-transfected cells (siUGDH + EPI vs. EPI **p < 0.05*) (Fig. 2A and 2B). Moreover, it was observed two well-differentiated populations of MDA-MB-231 cells in terms of EPI accumulation only when cells were transfected with siUGDH before being treated with EPI (siUGDH + EPI), as it could observed in the flow cytometry analysis. These results were not found in the treatments carried out with EPI (EPI) or in MDA-MB-231 cells transfected with siSCR (siSCR + EPI) (Fig. 2C). Considering these previous results, we decided to continue evaluating possible mechanisms involved in the development of drug resistance.

Modulation of expression of genes of drug efflux pumps and its inactivation after UGDH knockdown and EPI treatment.

To understand possible mechanisms that involve the evasion of EPI antitumoral effects despite its higher cell accumulation, we analyzed the expression of different genes related to the drug inactivation.

Since the silencing of UGDH affected the intracellular accumulation of EPI, this could be related to possible changes in the expression of drug efflux pumps implicated in EPI elimination. For that reason, we started analyzing the expression of different ATP-binding cassette (ABC) drug transporters implicated in EPI efflux: ABCG2, ABCC1 and ABCC2. We found a significant increase in mRNA levels in response to EPI treatment compared with basal conditions (EPI vs. BASAL: ABCG2 and ABCC1 **p < 0.05;* ABCC2 ***p < 0.01;* Fig. 3A, 3B, 3C). Nevertheless, the silencing of UGDH enzyme (siUGDH) as well as the combination with EPI treatment (siUGDH + EPI) did not induce a significant modulation of their expression compared to basal conditions or EPI treatment (Fig. 3A). These data could explain the increased intracellular accumulation of EPI after siUGDH transfection; however, these data are controversial regarding the results observed for the apoptosis process, indicating that an increase in EPI intracellular accumulation is not directly associated with an increase in cell death.

On the other hand, the UGT2B7 enzyme is the exclusive transferase responsible for binding EPI to UDP-GlcUA. As previously reported [12], after EPI treatment we found a significant up-regulation in the expression of the UGT2B7 compared to basal conditions (EPI vs. BASAL ***p < 0.01* Fig. 3D). Even more, we observed increased levels when breast cancer cells were transfected with siUGDH before treating them with EPI (siUGDH + EPI) (Fig. 3D). This result indicated that, although EPI efflux was not completely activated, tumor cells upregulated the expression of this enzyme in response to EPI treatment, as a new mechanism of drug resistance. Specifically, we can hypothesize that MDA-MB-231 increase UGT2B7 levels trying to increase the inactivation or elimination of EPI and avoid the antitumoral effect of this drug.

Effect of UGDH knockdown and EPI treatment on tumor angiogenesis, cell proliferation and migration

Among mechanisms involved in drug resistance, we have been previously reported that during chemotherapy treatment tumor cells can modulate angiogenesis, altering the behavior of endothelial cells. Tumor cells can secrete different pro-angiogenic factors such as VEGF, FGF-2, EGF, among others [33–35] capable of promoting the migration of endothelial cells and the formation of blood vessels. For that reason, we analyzed the mRNA expression levels of VEGF and EGF after UGDH knockdown and EPI treatment. We observed a significant increase in the expression of VEGF after treating tumor cells with EPI (EPI vs. BASAL ***p < 0.01* Fig. 4A). In turn, we observed even higher levels of VEGF mRNA when MDA-MB-231 cells were first transfected with UGDH siRNA and treated with EPI (EPI vs. siUGDH + EPI ***p < 0.01* Fig. 4A). In case of EGF, we found a similar tendency of up-regulation in response to EPI treatment; however, we only obtained statistically significant differences when cells were transfected with siUGDH and treated with EPI respect with transfected cells non-treated with EPI (siUGDH + EPI vs. siUGDH **p < 0.05* Fig. 4B).

Afterward, we analyzed the biosynthesis and secretion levels of VEGF by ELISA. We did not observe significant changes in VEGF concentration in supernatants from MDA-MB-231 cells transfected with siUGDH and treated with EPI (Fig. 4C). Considering that no differences were detected in VEGF protein levels in supernatants of tumor cells, other factors could be involved in tumor angiogenesis and be related to aggressive phenotypes of different types of cancer cells [36–38]. FGF-2 is a potent cell survival factor involved in tumor angiogenesis [38, 39] thus, we decided to evaluate FGF-2 biosynthesis. First, we analyzed FGF-2 protein expression by using supernatants from MDA-MB-231 that have been transfected with siUGDH and treated with EPI. However, no detectable levels were found by ELISA (data not shown). Since FGF-2 is not frequently detected into the medium of cultured cells because remains associated with cell-surface heparan sulfate proteoglycans upon secretion [40–42], we performed the ELISA with total cellular protein extract and we were able to detect it. However, we did not find significant differences between treatment and basal conditions at the time of the assay (Fig. 4D). These results could be associated to the fact that both samples were collected at the same time and the effect at the protein level should be analyzed later than the mRNA level.

On the other hand, tumor cells can avoid antitumoral treatment and generate drug resistance by the modulation of specific signaling pathways related to cell survival and proliferation. In this sense, we

decided to analyze a possible modulation in Wnt/β-catenin and PI3K/Akt pathways after the UGDH knockdown and EPI treatment. The expression of β-catenin and p-Akt proteins was analyzed by western blot from total protein extracts. When β-catenin was evaluated, we observed a tendency to increase the expression levels in response to the silencing of the UGDH enzyme. However, we did not find significant differences in comparison to basal conditions or EPI treatment (Fig. 4E). Finally, when we studied the expression of the active form of Akt (p-Akt), we found a similar tendency to that of β-catenin, but we did not find significant differences between treatments (Fig. 4F).

Subsequently, the migration ability of tumor cells has been determined as another process that indicates drug resistance and their ability to spread during chemotherapy. We observed that in response to EPI treatment, MDA-MB-231 cells increased their migration compared to basal conditions (EPI vs. BASAL ****p < 0.001)* (Fig. 4G and 4H). The same effect was observed when we analyzed the silencing of UGDH and posterior EPI treatment (siUGDH + EPI vs. BASAL **p < 0.05)* (Fig. 4G and 4H). These results are in concordance with the aggressive features of this cell line and their capacity to develop EPI resistance.

Effect of UGDH knockdown and EPI treatment on autophagy

Recent studies have shown that autophagy can protect cancer cell from antitumoral drug-induced death so that autophagy might be related to the development of drug resistance to these agents [43]. For that reason, we decided to study the modulation of autophagy as a possible mechanism involved in EPI resistance in breast cancer cells transfected with UGDH siRNA. First, we evaluated the mRNA expression of the autophagosome marker, LC3-II (Fig. 5A). We observed an up-regulation of LC3-II levels in response to EPI treatment compared with basal conditions (EPI vs. BASAL ****p < 0.001*). We also found an increase in LC3-II expression when MDA-MB-231 cells were transfected with UGDH siRNA and after that treated with EPI, compared to UGDH siRNA alone (Fig. 5A).

Since the differences found in the expression of LC3-II indicated a possible positive modulation of autophagy in response to EPI treatment, we decided to continue analyzing the formation of autophagosomes in tumor cells after UGDH silencing and treatment with EPI. A co-transfection system with the specific siRNAs (UGDH or SCR) was carried out together with an expression vector of a fusion protein LC3-II-GFP (green fluorescent protein) (Fig. 5B and 5C). In line with the above results, we detected an increase in the formation of autophagosomes in response to antitumor treatment with EPI compared with basal control (EPI vs. BASAL *****p < 0.0001*). Even more, we found increased levels of LC3-II positive-autophagosomes in MDA-MB-231 cells that have been first silenced for UGDH and after that, treated with EPI. These results were confirmed through the analysis of the protein expression of LC3-I and LC3-II by western blot. We found that LC3-II levels were even higher when the UGDH enzyme was silenced before treating tumor cells with EPI (Fig. 5D). Taken together, these results would indicate that breast cancer cells respond to EPI treatment favoring tumor survival and adaptation to the stress generated by the antitumor treatment. Moreover, we observe that the lack of UGDH enzyme could support the development of resistance to EPI through the process of autophagy. Both the western blot and the GFP-LC3 experiments were performed using chloroquine, a specific inhibitor of autophagy, as negative control (data not shown).

Effect of UGDH knockdown and EPI treatment on extracellular matrix and HA expression

Since UDP-GlcUA is a precursor for the synthesis of several GAGs and PGs, and the silencing of the UGDH enzyme can modulate its production, we continued studying the effect of UGDH knockdown and EPI treatment on the ECM and its components. To evaluate the ability of tumor cells to generate an interstitial or pericellular matrix, a particle exclusion assay was performed in MDA-MB-231 cells during UGDH siRNA transfection and EPI treatment. Surprisingly, we observed that the pericellular area of MDA-MB-231 cells remained similar to basal conditions when the UGDH enzyme was silenced (Fig. 6A and 6B). When tumor cells were treated only with EPI as a control, a significant increase in the pericellular area was observed in comparison to basal conditions (EPI vs. BASAL ***$p < 0.001$). This effect was also observed and even more increased, when tumor cells were treated with EPI after UGDH knockdown, compared to the effect produced by EPI (siUGDH + EPI vs. EPI ***$p < 0.001$) (Fig. 6A and 6B). The inclusion of a specific control with a hyaluronidase enzyme during the assay (HYAL), allowed us to estimate which fraction of this pericellular matrix is composed of HA. In this case, when tumor cells were treated with HYAL before the addition of the red blood cells, a small pericellular area was observed, with statistically significant decrease respect to basal conditions (HYAL vs. BASAL ***$p < 0.001$) (Fig. 6A and 6B). All these data indicate that after UGDH knockdown, although MDA-MB-231 cells had a diminished availability of UGDH enzyme to synthesize UDP-GlcUA, they were able to favor the expression GAGs within the ECM components in this condition. Moreover, it was demonstrated that the pericellular matrix of these tumor cells was mainly composed of HA.

Moreover, it is known that not all synthesized HA remains in the plasma membrane. HA chains can be released to cell media during the culture of tumor cells. To determine the levels of HA that were secreted to the cell medium, we performed an ELISA like-assay using a specific HA binding protein (HABP). In this case, we did not observe significant differences in HA secretion under UGDH knockdown or EPI treatment (Fig. 6C). We only detected a slight tendency to increase HA concentration when the tumor cells were transfected with the specific siRNA against UGDH (siUGDH vs. BASAL) (Fig. 6C).

Modulation of HA metabolism: a balance between HASes and HYALs

To continue analyzing the modulation of HA synthesis, under the silencing of UGDH and the treatment with EPI, we decided to investigate a possible association between the results previously obtained and HA metabolism. For that reason, we evaluated the mRNA expression of the i) synthesizing enzymes of HA: HAS-2 (Fig. 6D) and HAS-3 (Fig. 6E) and ii) HA degrading enzymes: HYAL-1 (Fig. 6F), HYAL-2 (Fig. 6G) and HYAL-3 (Fig. 6H). When we analyzed the expression levels of HAS-2 and HAS-3, we observed an increase in the expression of both enzymes in response to EPI treatment (EPI vs. BASAL *$p < 0.05$) (Fig. 6D and 6E). In turn, the silencing of UGDH enzyme combined with EPI treatment further increased the expression levels of both enzymes in comparison with basal control (Fig. 6D and 6E). Since these results are in line with the data obtained in the particle exclusion assay and the HA ELISA like-assay, considering that HAS-3 is responsible for synthesizing the HA that is generally retained in the plasma membrane. At the same time, HAS-2 is mostly involved in the synthesis of HA released into the cellular medium [44].

Furthermore, the expression of the main HA degrading enzymes were analyzed. In all cases, we observed a similar pattern of increase in the expression of the three enzymes, where EPI *per se* was able to upregulate the expression of the three HYALs compared to basal conditions (Fig. 6F, 6G and 6H). Furthermore, we found even higher expression levels of HYALs when MDA-MB-231 cells were first transfected with siUGDH and subsequently treated with EPI (Fig. 6F, 6G and 6H). Taking together these results, we can conclude that even under the silencing of an enzyme involved in HA synthesis and an antitumoral treatment such us EPI, MDA-MB-231 breast cancer cells were able to favor the synthesis of this GAG. Even more, tumor cells responded to both conditions augmenting ECM deposition as another mechanism of tumor drug resistance.

Discussion

During the last decades, EPI has been considered one of the most active drugs used in the treatment of breast cancer resistant to hormonal therapy [2]. EPI is a semisynthetic derivative of DOX anthracycline that produces similar efficacy with less adverse effects. This effect is due to a differential elimination mechanism than observed in DOX, through a 4-O-glucuronidation reaction [5, 6]. This reaction occurs mainly in the liver, where the enzyme UGT2B7 transfers a molecule of UDP-GlcUA to EPI [9]. It has been shown that, in hepatocellular carcinoma cells, the expression of this enzyme is tightly regulated by EPI treatment through the p53 pathway [12]. In turn, different studies have analyzed the role of UGDH as a marker of tumor progression during chemotherapy with drugs that are eliminated by glucuronidation. Since it generates the UDP-GlcUA substrate hence the activity of these enzymes is related to glucose metabolism and the synthesis of GAGs and PGs [45, 46]. UGDH enzyme transforms UDP-glucose (UDP-Glc) into UDP-GlcUA, a substrate of the specific enzymes that synthesize HA.

Although UGDH knockdown strategies have been proposed to evaluate the role of a potential modulator of breast cancer progression [47], in the present work, we studied for the first time the expression of this enzyme using MDA-MB-231, a breast adenocarcinoma cell line. Furthermore, we evaluated the role of UGDH during chemotherapy treatment with EPI. We have observed that MDA-MB-231 cells express the UGDH enzyme, and we have found a similar effect to that previously reported [13], where the expression was positively regulated in response to EPI treatment. The up-regulation of the expression of UGDH could promote the elimination of this cytotoxic drug from tumor cells. It could be related to an increased demand of UDP-GlcUA, which is crucial to conjugate EPI and promote its elimination, avoiding its action. Besides, in lung cancer, it has been proposed that an increase in the expression or availability of this enzyme might favor metastasis. This process occurs through the specific interaction between UGDH and HuR protein, which attenuates the UDP-Glc-mediated inhibition of the association of HuR with SNAI1 mRNA, stabilizing it. Increased production of SNAIL initiates the epithelial-mesenchymal transition, thus promoting the migration of tumor cells and metastasis [48].

The key point in our study was to investigate the effect of silencing UGDH enzyme on the antitumoral activity of EPI, and the response induced in breast cancer cells in terms of pro-tumoral processes, such as apoptosis, proliferation, migration and angiogenesis. On the other hand, we studied its association with

the generation of an ECM that favors tumor development and resistance. In the present work, we observed that silencing of UGDH enzyme combined with EPI treatment did not modified cell viability or cytotoxicity, which means that a possible modulation in the behavior of MDA-MB-231 cells might be a consequence of the effect of reducing the expression of UGDH. We only found significant differences in apoptosis induction after the silencing of UGDH, which seems to diminish the functional ability of EPI as a cytotoxic drug. Contrary to our expectations, we found a significant decrease in the induction of apoptosis in MDA-MB-231 breast cancer cells that have been transfected with siUGDH and after that, treated with EPI.

Although MDA-MB-231 cells transfected with siUGDH accumulated a higher amount of EPI, it was not enough to increase the levels of apoptosis observed in the same conditions, moreover apoptosis significantly decreased. These results could be associated with the fact that after silencing UGDH, there is less enzyme available to produce UDP-GlcUA, and UDP-GlcUA will be found in a reduced proportion inside tumor cells. For that reason, there would be less EPI glucuronidation that what is necessary to eliminate the drug. One possible explanation for this result is that intracellular accumulation of EPI does not reflect a full activity of this drug or its location is different inside the cell. Thus, we can hypothesize that despite unconjugated EPI; it is out to the nucleus, avoidance its activities as a DNA intercalant and finally its antitumoral action. Another alternative reason could be that EPI is in its inactive form that is conjugated to UDP-GlcUA. However, we could not detect it because the inactive forms of anthracyclines are also capable of emitting the same fluorescence intensity as the free-ones.

It is important to highlight that we found two well-differentiated populations of tumor cells with different ability to accumulate EPI after silencing the UGDH enzyme. This result supports our hypothesis, indicating that the population with the less accumulation of EPI presents resistant characteristics that favor EPI inactivation and contribute to the whole resistant-phenotype observed in our experiments. These results were unexpected, and different studies will be required to analyze and evaluate each population, which will be carried out as an extension of the present study.

We continued evaluating the expression of drug efflux pumps and the specific transferase involved in EPI inactivation as correlators of a possible mechanism of drug resistance [49–51]. As was expected, EPI treatment upregulated the expression of drug efflux pumps; however, the silencing of UGDH plus EPI treatment did not induce a significant modulation of their expression. In turn, a significant increase in the expression of the UGT2B7 transferase was observed in response to UGDH knockdown and EPI treatment. These results indicate that, although EPI efflux was not completely activated, tumor cells upregulated the expression of this enzyme in order to improve the elimination of EPI and avoid the antitumoral effect of this drug.

All these data, plus the decrease in apoptosis as opposed to a higher EPI accumulation, allow us to hypothesize that MDA-MB-231 cells have succeeded in avoiding the potential effect of higher accumulating EPI, favoring mechanisms to develop drug resistance and tumor progress during the antitumoral treatment with EPI. In fact, several previous studies have suggested that the appearance of

resistance to EPI can occur through different mechanisms, including resistance mediated by P-glycoprotein, changes in the activity of topoisomerase II, inhibition of apoptotic pathways, among others [49–52].

Within mechanisms involved in the development of drug resistance are the modulation of specific processes related to cell survival, proliferation and migration [27, 49], as well as tumor angiogenesis [36]. We found a slight increase in β-catenin and p-Akt protein levels in response to UGDH knockdown. However, we did not observe any difference in the activation of these signaling pathways with the addition of EPI. On the contrary, a significant pro-tumoral effect was visualized in response to the silencing of the UGDH enzyme when analyzing angiogenesis and tumor migration. In this sense, we observed an increase in the expression of both pro-angiogenic factors VEGF and FGF-2 when cells were transfected with siUGDH and after that, treated with EPI, which are closely involved in the activation angiogenesis in the tumor environment [36]. In turn, we observed that tumor cells not only conserved their migratory ability under those conditions but also increased their migration even under the silencing of the UGDH enzyme and EPI treatment. Moreover, could be explain that the migratory capacity are associated with HA synthesis and degradation, as was observed changes in the expression of HAS and HYAL enzymes [53]. Together, these results indicate that, despite being under an antitumoral treatment and with less availability of the UGDH enzyme, tumor cells activated several mechanisms directly related to tumor progression and drug resistance, despite the cells were reducing its glucuronidation and elimination.

One of the processes recently discovered to be involved with EPI resistance is autophagy. Some evidences indicate that cell autophagy protects MCF-7 breast cancer cells from EPI-induced apoptosis and facilitates the development of EPI resistance that acts as a cell survival factor [13]. In fact, in the present study, positive modulation of the autophagy process has been demonstrated in response to EPI treatment, as previously explained. Even more, that effect was also observed in response to UGDH silencing and subsequent EPI treatment. Taken together, these results would indicate that breast cancer cells favor tumor survival and adaptation to the stress generated by the antitumoral treatment with EPI. Moreover, we observe that the lack of UGDH enzyme could support the development of resistance to EPI through the process of autophagy.

Furthermore, we consider important to highlight that tumor cells are able to modulate their extracellular microenvironment to avoid drug action [54]. According to the role of UGDH enzyme in HA expression, there are controversial data regarding the effect on the modulation of its expression. First, it has been demonstrated that a diminished function of the UGDH enzyme (either by siRNA or 4-MU, which affects the levels of UDP-GlcUA), in aortic smooth muscle cells [14] and human keratinocytes [55], significantly reduces the production of HA. According to that previous results, *Wang et al.* demonstrated that inhibition of UGDH expression significantly decreased the invasive capacity of HCT-8 colorectal carcinoma cells in combination with a reduction in the expression of different GAGs. However, the experiments were carried out without a chemotherapeutic agent, such as an anthracycline. However, we analyzed the effect of UGDH knockdown plus treatment with EPI on the metabolism of HA and the appearance of drug resistance. Although we observed that MDA-MB-231 cells had less availability of UGDH enzyme to

synthesize UDP-GlcUA, cells were able to favor the expression of ECM components mainly composed of HA. However, we found no differences in the concentration of HA present in the cellular medium. We continue analyzing the expression of HAS and HYAL enzymes as essential components of HA metabolism. The silencing of UGDH combined with EPI treatment increased the expression of HAS-2 and HAS-3, closely related to results observed in the pericellular area and HA secreted to the cellular microenvironment.

Conversely, we observed less increase in HAS-2 expression in accordance with a slight modulation of soluble HA levels. Besides, it would be interesting to study the molecular weight of HA produced by tumor cells, since it can have differentiated functions [22]. Furthermore, the unexpected increase in HYALs expression considering higher pericellular area could be explained taking into account that, in the absence of UGDH enzyme, breast cancer cells require a new source of UDP-GlcUA to synthesize HA (and other GAGs and PGs). Consequently, MDA-MB-231 cells could activate the synthesis of the enzymes that degrade HA to favor this process, since it can digest its precursors, leaving them available for other processes, such as, EPI glucuronidation.

Our results are in line with previous studies in prostate cancer, where it was shown that when overexpressing the UGDH enzyme during androgen treatment (similarly eliminated by glucuronidation), the synthesis of HA was not stimulated, although HAS-3 expression was increased [46]. However, it has been determined that sugars attached to UDP (UDP-sugars) influence the transport of HAS-3 to the plasma membrane of melanoma cells, thereby affecting the function of that enzyme and finally, HA synthesis [56–59]. In fact, the synthesis of this GAG can be regulated by cell metabolism because glucose levels have a substantial impact on the concentration of UDP-sugars. Therefore, it would be important to determine the activity of HYALs enzymes, as well as the analysis of UDP-sugars available in MDA-MB-231 cells in order to determine whether the increase in the expression implicates an increase in the activity of enzymes.

Conclusion. In the present work we have demonstrated the role of the UGDH enzyme during the antitumoral treatment with the anthracycline EPI, Even more, we proposed a new mechanism of resistance to chemotherapy that involves a close relationship between the modulation of the ECM and the inactivation of the EPI. MDA-MB-231 breast cancer cells shown less availability of UGDH enzyme to synthesize UDP-GlcUA, responsible for EPI elimination. While a decrease in the availability of UDP-GlcUA resulted in an increase in the intracellular accumulation of EPI, tumor cells have succeeded in avoiding the potential effect of higher accumulating EPI. MDA-MB-231 cells promoted mechanisms related to the development of drug resistance, such as the up-regulation of the expression of efflux pumps as well as autophagy. In turn, MDA-MB-231 cells were able to favor the expression of ECM components, mainly composed of HA, which could also contribute to the development of resistance to EPI. To sum up, we suggest that a specific tumor microenvironment and ECM favorable to the intracellular accumulation of EPI would not necessarily increase the activity of the drug, and the consequent efficiency of the chemotherapy treatment. Tumor cells demonstrated to be able to respond negatively to EPI treatment by

activating crucial cellular processes as angiogenesis and cell migration and by leading to the re-organization of ECM components such as HA, which favors tumor progression (Fig. 7).

Abbreviations

DOX: doxorubicin

EPI: epirubicin

UGT: UDP-glucuronosyltransferase

UDP-GlcUA: UDP-glucuronic acid

GAG: glycosaminoglycan

ECM: extracellular matrix

HA: hyaluronan

PG: proteoglycan

siRNA: small interference RNA

4-MU: 4-methylumbelliferone

Declarations

ETHICS APPROVAL AND CONSENT TO PARTICIPATE

Not applicable

CONSENT FOR PUBLICATION

Not aplicable

AVAILABILITY OF DATA AND MATERIALS

The authors declare that all data supporting the findings of this study are available within the article. Besides, the datasets generated during and/or analyzed during the current study are available from the corresponding author on reasonable request (laualaniz@comunidad.unnoba.edu.ar).

COMPETING INTERESTS

The authors declare that they have no competing interests

FUNDING

This work was supported by H2020 RISE-MSCA Project grant number 645756 (GLYCANC) (to Alaniz L. and Passi. A). SIB 0561/2019, UNNOBA (to Alaniz L). All the authors indicate no potential conflicts of interest.

AUTHORS' CONTRIBUTIONS

D.L.V. performed and conducted the experiments, analyzed the data, designed the figures and wrote the paper; I.C. and Ar.P. performed the confocal microscopy, western blot experiments and manuscript revision; I.S., F.M.S. and A.I. collaborated with experiments and analyzed data. A.P. contributed with essential manuscript revision. D.V. and L.A. conceived and designed the research, supervise the experiments, analyzed the data, and wrote the paper. All authors read and approved the final manuscript.

ACKNOWLEDGMENTS

The authors thank Natalia Menite for expert technical assistance in flow cytometry

AUTHORS' INFORMATION

D.L.V, F.M. S. and A. I. are PhD fellow at National Scientific and Technical Research Council (CONICET), Argentina.

Ar. P. is a PhD student of the “Life Science and Biotechnology” course at Università degli studi dell’Insubria. Italy

I.S. is a posdoc fellow at CONICET. Argentina.

A.P. MD, PhD, Full Professor of biochemistry Department of Surgical and Morphological Sciences (DSCM). School of Medicine, University of Insubria, Varese, Italy

D.V. Ph.D., Associate professor of biochemistry DSCM. School of Medicine, University of Insubria, Varese, Italy.

L.A. Ph.D., independent researcher at CONICET. Associate professor of School of Agrarian, Natural and Environmental (ECANA). National University of the Northwest of the Province of Bs. As. Argentina.

References

1. Weiss, R.B., *The anthracyclines: will we ever find a better doxorubicin?* Semin Oncol, 1992. **19**(6): p. 670-86.
2. Coukell, A.J. and D. Faulds, *Epirubicin. An updated review of its pharmacodynamic and pharmacokinetic properties and therapeutic efficacy in the management of breast cancer.* Drugs, 1997. **53**(3): p. 453-82.

3. Foulkes, W.D., I.E. Smith, and J.S. Reis-Filho, *Triple-negative breast cancer.* N Engl J Med, 2010. **363**(20): p. 1938-48.
4. Ormrod, D., et al., *Epirubicin: a review of its efficacy as adjuvant therapy and in the treatment of metastatic disease in breast cancer.* Drugs Aging, 1999. **15**(5): p. 389-416.
5. Robert, J. and L. Gianni, *Pharmacokinetics and metabolism of anthracyclines.* Cancer Surv, 1993. **17**: p. 219-52.
6. Danesi, R., et al., *Pharmacokinetic-pharmacodynamic relationships of the anthracycline anticancer drugs.* Clin Pharmacokinet, 2002. **41**(6): p. 431-44.
7. Camaggi, C.M., et al., *Biliary excretion and pharmacokinetics of 4'epidoxorubicin (epirubicin) in advanced cancer patients.* Cancer Chemother Pharmacol, 1986. **18**(1): p. 47-50.
8. Mackenzie, P.I., et al., *The UDP glycosyltransferase gene superfamily: recommended nomenclature update based on evolutionary divergence.* Pharmacogenetics, 1997. **7**(4): p. 255-69.
9. Innocenti, F., et al., *Epirubicin glucuronidation is catalyzed by human UDP-glucuronosyltransferase 2B7.* Drug Metab Dispos, 2001. **29**(5): p. 686-92.
10. Plosker, G.L. and D. Faulds, *Epirubicin. A review of its pharmacodynamic and pharmacokinetic properties, and therapeutic use in cancer chemotherapy.* Drugs, 1993. **45**(5): p. 788-856.
11. Ravdin, P.M., *Anthracycline resistance in breast cancer: clinical applications of current knowledge.* Eur J Cancer, 1995. **31A Suppl 7**: p. S11-4.
12. Hu, D.G., A. Rogers, and P.I. Mackenzie, *Epirubicin upregulates UDP glucuronosyltransferase 2B7 expression in liver cancer cells via the p53 pathway.* Mol Pharmacol, 2014. **85**(6): p. 887-97.
13. Sun, W.L., et al., *Autophagy protects breast cancer cells from epirubicin-induced apoptosis and facilitates epirubicin-resistance development.* Autophagy, 2011. **7**(9): p. 1035-44.
14. Vigetti, D., et al., *Molecular cloning and characterization of UDP-glucose dehydrogenase from the amphibian Xenopus laevis and its involvement in hyaluronan synthesis.* J Biol Chem, 2006. **281**(12): p. 8254-63.
15. Caon, I., et al., *Cell Energy Metabolism and Hyaluronan Synthesis.* J Histochem Cytochem, 2020: p. 22155420929772.
16. Tukey, R.H. and C.P. Strassburg, *Human UDP-glucuronosyltransferases: metabolism, expression, and disease.* Annu Rev Pharmacol Toxicol, 2000. **40**: p. 581-616.
17. Vigetti, D., et al., *Hyaluronan: biosynthesis and signaling.* Biochim Biophys Acta, 2014. **1840**(8): p. 2452-9.
18. Prydz, K. and K.T. Dalen, *Synthesis and sorting of proteoglycans.* J Cell Sci, 2000. **113 Pt 2**: p. 193-205.
19. Gotte, M. and G.W. Yip, *Heparanase, hyaluronan, and CD44 in cancers: a breast carcinoma perspective.* Cancer Res, 2006. **66**(21): p. 10233-7.
20. Spinelli, F.M., et al., *The immunological effect of hyaluronan in tumor angiogenesis.* Clin Transl Immunology, 2015. **4**(12): p. e52.

21. Itano, N. and K. Kimata, *Altered hyaluronan biosynthesis in cancer progression.* Semin Cancer Biol, 2008. **18**(4): p. 268-74.
22. Tavianatou, A.G., et al., *Hyaluronan: molecular size-dependent signaling and biological functions in inflammation and cancer.* FEBS J, 2019. **286**(15): p. 2883-2908.
23. Caon, I., et al., *Revisiting the hallmarks of cancer: The role of hyaluronan.* Semin Cancer Biol, 2020. **62**: p. 9-19.
24. Viola, M., et al., *MDA-MB-231 breast cancer cell viability, motility and matrix adhesion are regulated by a complex interplay of heparan sulfate, chondroitin-/dermatan sulfate and hyaluronan biosynthesis.* Glycoconj J, 2017. **34**(3): p. 411-420.
25. Spinelli, F.M., et al., *Hyaluronan preconditioning of monocytes/macrophages affects their angiogenic behavior and regulation of TSG-6 expression in a tumor type-specific manner.* FEBS J, 2019. **286**(17): p. 3433-3449.
26. Huang, D., et al., *Udp-glucose dehydrogenase as a novel field-specific candidate biomarker of prostate cancer.* Int J Cancer, 2010. **126**(2): p. 315-27.
27. Vitale, D.L., et al., *Co-treatment of tumor cells with hyaluronan plus doxorubicin affects endothelial cell behavior independently of VEGF expression.* Oncotarget, 2018. **9**(93): p. 36585-36602.
28. Alaniz, L., et al., *Low molecular weight hyaluronan inhibits colorectal carcinoma growth by decreasing tumor cell proliferation and stimulating immune response.* Cancer Lett, 2009. **278**(1): p. 9-16.
29. Schagger, H., *Tricine-SDS-PAGE.* Nat Protoc, 2006. **1**(1): p. 16-22.
30. Liang, C.C., A.Y. Park, and J.L. Guan, *In vitro scratch assay: a convenient and inexpensive method for analysis of cell migration in vitro.* Nat Protoc, 2007. **2**(2): p. 329-33.
31. Caon, I., et al., *Sirtuin 1 reduces hyaluronan synthase 2 expression by inhibiting nuclear translocation of NF-kappaB and expression of the long-noncoding RNA HAS2-AS1.* J Biol Chem, 2020. **295**(11): p. 3485-3496.
32. Piccioni, F., et al., *4-methylumbelliferone inhibits hepatocellular carcinoma growth by decreasing IL-6 production and angiogenesis.* Glycobiology, 2015. **25**(8): p. 825-35.
33. Carmeliet, P., *VEGF as a key mediator of angiogenesis in cancer.* Oncology, 2005. **69 Suppl 3**: p. 4-10.
34. Ferrara, N., *The role of VEGF in the regulation of physiological and pathological angiogenesis.* EXS, 2005(94): p. 209-31.
35. Chung, A.S. and N. Ferrara, *Developmental and pathological angiogenesis.* Annu Rev Cell Dev Biol, 2011. **27**: p. 563-84.
36. Ziyad, S. and M.L. Iruela-Arispe, *Molecular mechanisms of tumor angiogenesis.* Genes Cancer, 2011. **2**(12): p. 1085-96.
37. Xu, Q., et al., *EGF induces epithelial-mesenchymal transition and cancer stem-like cell properties in human oral cancer cells via promoting Warburg effect.* Oncotarget, 2017. **8**(6): p. 9557-9571.

38. Barclay, C., et al., *Basic fibroblast growth factor (FGF-2) overexpression is a risk factor for esophageal cancer recurrence and reduced survival, which is ameliorated by coexpression of the FGF-2 antisense gene.* Clin Cancer Res, 2005. **11**(21): p. 7683-91.
39. Polnaszek, N., et al., *Fibroblast growth factor 2 promotes tumor progression in an autochthonous mouse model of prostate cancer.* Cancer Res, 2003. **63**(18): p. 5754-60.
40. Trudel, C., et al., *Translocation of FGF2 to the cell surface without release into conditioned media.* J Cell Physiol, 2000. **185**(2): p. 260-8.
41. Zehe, C., et al., *Cell-surface heparan sulfate proteoglycans are essential components of the unconventional export machinery of FGF-2.* Proc Natl Acad Sci U S A, 2006. **103**(42): p. 15479-84.
42. Backhaus, R., et al., *Unconventional protein secretion: membrane translocation of FGF-2 does not require protein unfolding.* J Cell Sci, 2004. **117**(Pt 9): p. 1727-36.
43. Kondo, Y., et al., *The role of autophagy in cancer development and response to therapy.* Nat Rev Cancer, 2005. **5**(9): p. 726-34.
44. Itano, N., et al., *Selective expression and functional characteristics of three mammalian hyaluronan synthases in oncogenic malignant transformation.* J Biol Chem, 2004. **279**(18): p. 18679-87.
45. Wang, T.P., et al., *Down-regulation of UDP-glucose dehydrogenase affects glycosaminoglycans synthesis and motility in HCT-8 colorectal carcinoma cells.* Exp Cell Res, 2010. **316**(17): p. 2893-902.
46. Wei, Q., et al., *Androgen-stimulated UDP-glucose dehydrogenase expression limits prostate androgen availability without impacting hyaluronan levels.* Cancer Res, 2009. **69**(6): p. 2332-9.
47. Huh, J.W., et al., *Inhibition of human UDP-glucose dehydrogenase expression using siRNA expression vector in breast cancer cells.* Biotechnol Lett, 2005. **27**(16): p. 1229-32.
48. Wang, X., et al., *UDP-glucose accelerates SNAI1 mRNA decay and impairs lung cancer metastasis.* Nature, 2019. **571**(7763): p. 127-131.
49. Tredan, O., et al., *Drug resistance and the solid tumor microenvironment.* J Natl Cancer Inst, 2007. **99**(19): p. 1441-54.
50. Zhou, S., et al., *The ABC transporter Bcrp1/ABCG2 is expressed in a wide variety of stem cells and is a molecular determinant of the side-population phenotype.* Nat Med, 2001. **7**(9): p. 1028-34.
51. Gottesman, M.M., T. Fojo, and S.E. Bates, *Multidrug resistance in cancer: role of ATP-dependent transporters.* Nat Rev Cancer, 2002. **2**(1): p. 48-58.
52. Ravdin, P.M., *Reflections on the development of resistance during therapy for advanced breast cancer. Implications of high levels of activity of docetaxel in anthracycline-resistant breast cancer patients.* Eur J Cancer, 1997. **33 Suppl 7**: p. S7-10.
53. Tammi, M.I., et al., *Activated hyaluronan metabolism in the tumor matrix - Causes and consequences.* Matrix Biol, 2019. **78-79**: p. 147-164.
54. Mohan, V., A. Das, and I. Sagi, *Emerging roles of ECM remodeling processes in cancer.* Semin Cancer Biol, 2020. **62**: p. 192-200.

55. Rilla, K., et al., *The hyaluronan synthesis inhibitor 4-methylumbelliferone prevents keratinocyte activation and epidermal hyperproliferation induced by epidermal growth factor.* J Invest Dermatol, 2004. **123**(4): p. 708-14.
56. Deen, A.J., et al., *UDP-sugar substrates of HAS3 regulate its O-GlcNAcylation, intracellular traffic, extracellular shedding and correlate with melanoma progression.* Cell Mol Life Sci, 2016. **73**(16): p. 3183-204.
57. Vigetti, D. and A. Passi, *Hyaluronan synthases posttranslational regulation in cancer.* Adv Cancer Res, 2014. **123**: p. 95-119.
58. Passi, A., et al., *Dissecting the role of hyaluronan synthases in the tumor microenvironment.* FEBS J, 2019. **286**(15): p. 2937-2949.
59. Melero-Fernandez de Mera, R.M., et al., *Effects of mutations in the post-translational modification sites on the trafficking of hyaluronan synthase 2 (HAS2).* Matrix Biol, 2019. **80**: p. 85-103.

Figures

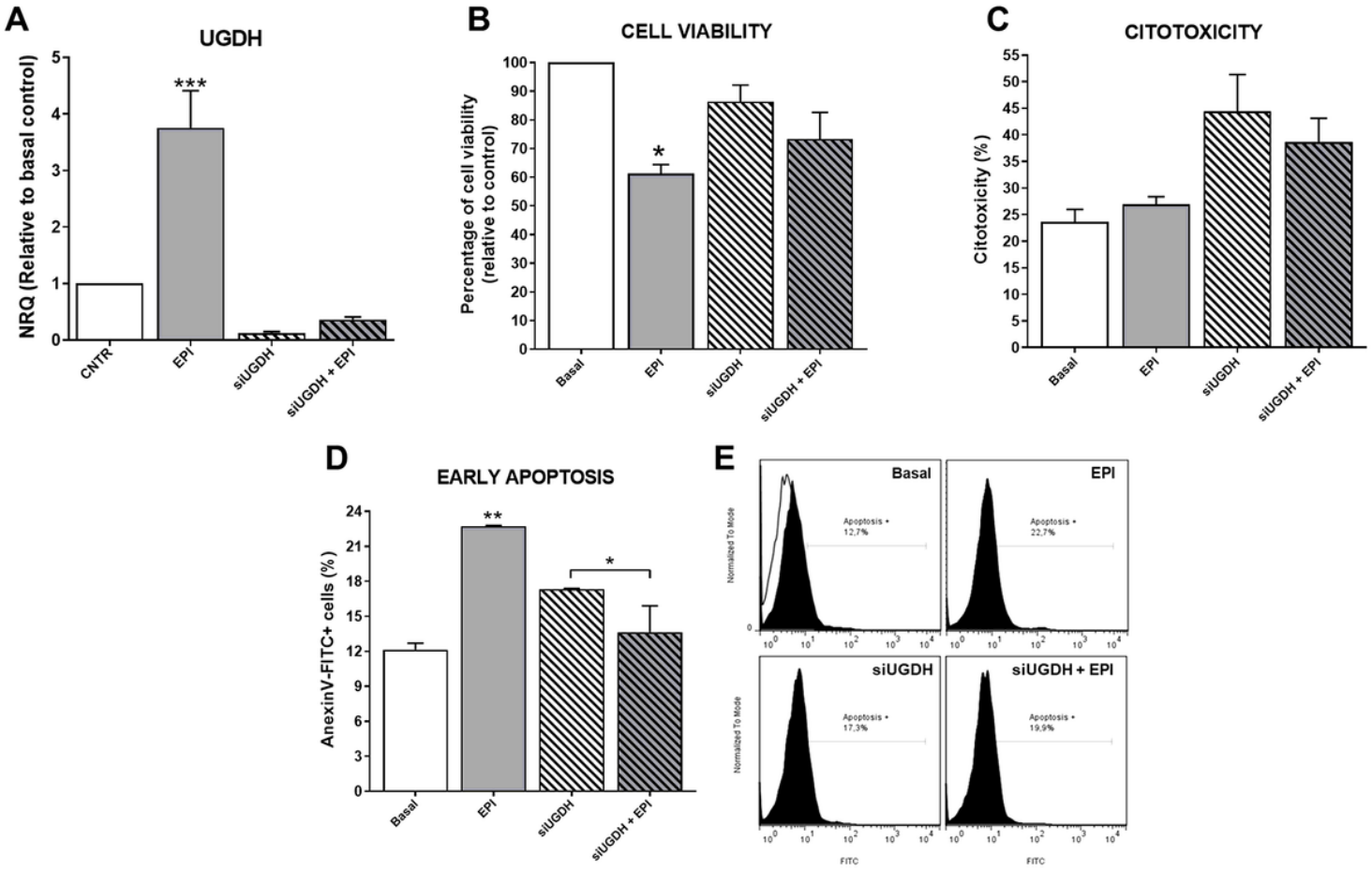

Figure 1

Analysis of MDA-MB-231 cells after silencing of UGDH gene and EPI treatment. MDA-MB-231 cells were transfected with a specific siRNA against UGDH gene (siUGDH) using a random sequence siRNA as

negative control (siSCR). After 24h, 1 μM EPI (1 EPI) was added to complete 48h of incubation. UGDH mRNA levels were obtained by real time quantitative PCR using Taqman® probes (A). Cell viability was measured performing a MTT assay (B) and cytotoxicity was determined evaluating the activity of lactate dehydrogenase (LDH) enzyme in cell supernatants (C). Early apoptosis (D and E) was detected by flow cytometry using AnnexinV-FICT stain. Histograms (E) show most representative of three independent experiments performed with 50,000 events/condition. N = 3, as mean ± SEM *p<0.05 **p<0.01.

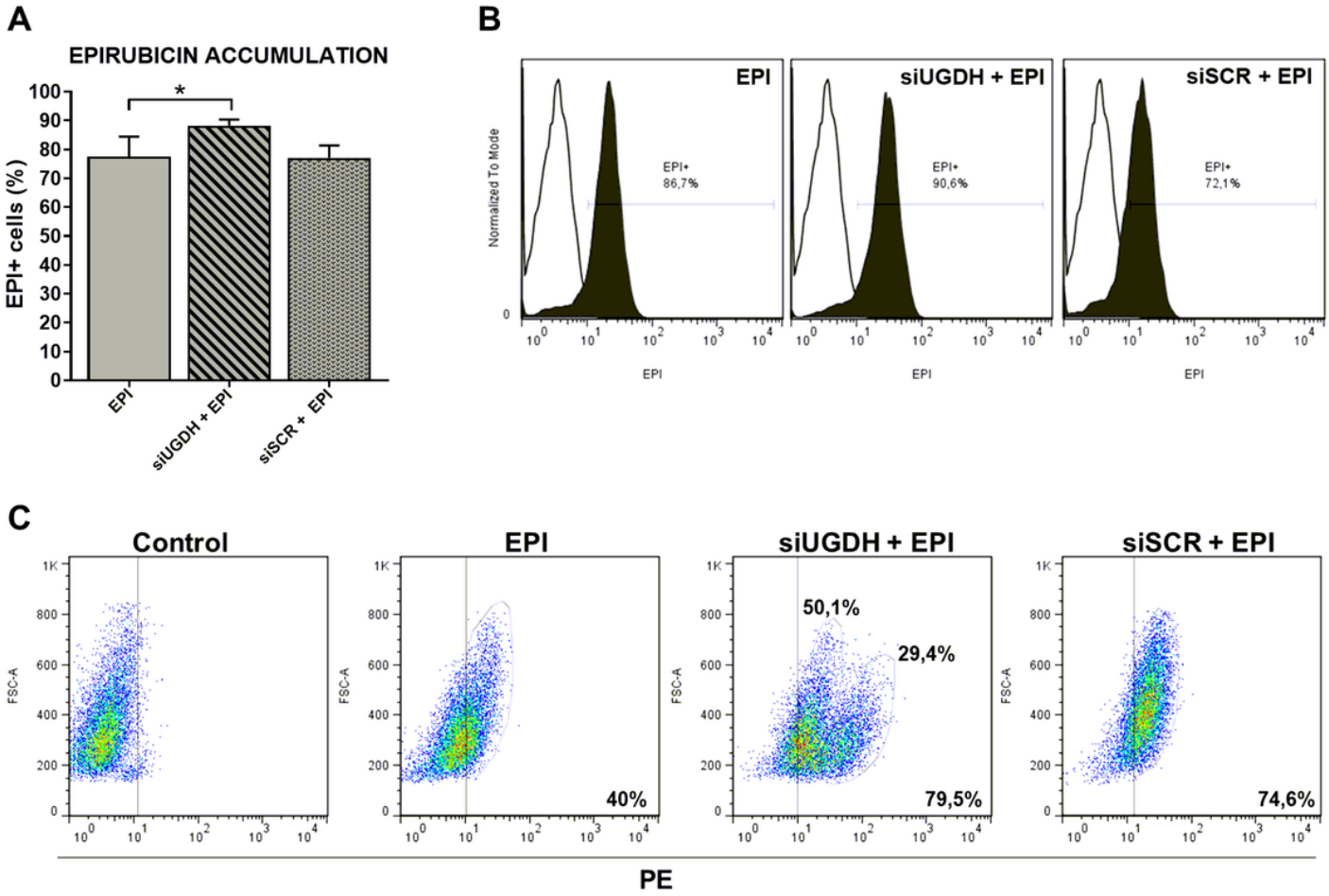

Figure 2

Evaluation of intracellular EPI accumulation in MDA-MB-231 cells after knockdown UGDH gene. MDA-MB-231 cells were transfected with a specific siRNA against UGDH gene (siUGDH) using a random sequence siRNA as negative control (siSCR). After 24h, 1 μM EPI (1 EPI) was added to complete 48h of incubation. Intracellular EPI accumulation was measured by flow cytometry. Bars show the percentage of EPI+ cells determined by comparison with a negative control (A). Histograms (B) and dot plots (C) show most representative of four independent experiments performed with 50,000 events/condition. N = 4, as mean ± SEM *p<0.05.

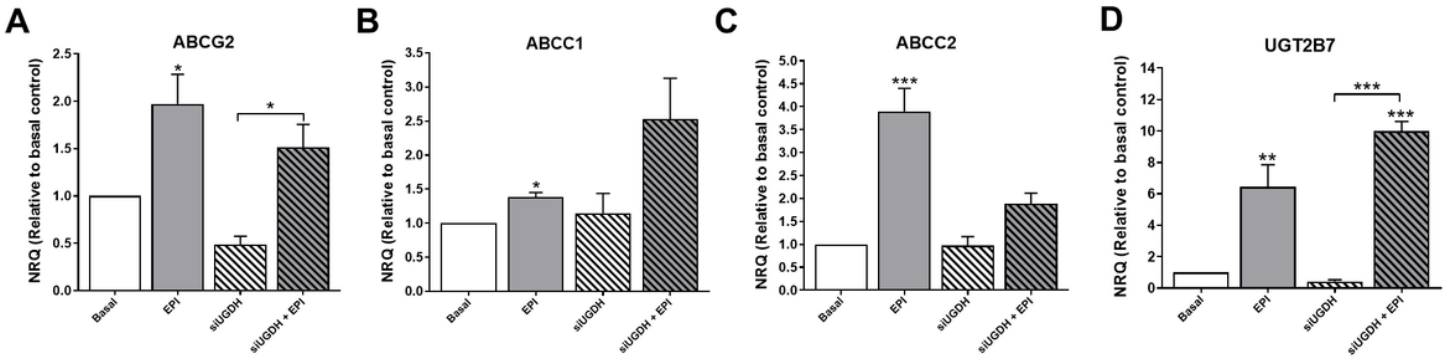

Figure 3

Analysis of drug resistance mechanisms as response of silencing UGDH enzyme and EPI treatment. MDA-MB-231 cells were transfected with a specific siRNA against UGDH gene (siUGDH) using a random sequence siRNA as negative control (siSCR). After 24h, 1 μM EPI (1 EPI) was added to complete 48h of incubation. To evaluate the expression of ABCG2 (A), ABCC1 (B), ABCC2 (C), and UGT2B7 (D), drug efflux pumps and the specific EPI transferase UGT2B7, total RNA was extracted and 2 μg were reverse transcribed by RT-PCR. cDNAs were subjected to real time quantitative PCR using SYBR Green. Results were normalized using β-actin as reference gene and all determinations were performed as duplicates. N = 3, as mean ± SEM *p<0.05 **p<0.01 ***p<0.001.

NOT PROVIDED WITH THIS VERSION

Figure 4

Evaluation of angiogenic response, cell proliferation and migration after silencing UGDH enzyme and EPI treatment. MDA-MB-231 cells were transfected with a specific siRNA against UGDH gene (siUGDH) using a random sequence siRNA as negative control (siSCR). After 24h, 1 μM EPI (1 EPI) was added to complete 48h of incubation. VEGF (A) and EGF (B) expression were obtained by real time quantitative PCR using SYBR Green. Results were normalized using β-actin as reference gene and all determinations were performed as duplicates. Levels of secreted VEGF in cell supernatants (C), and intracellular levels of FGF-2 in cell lysates (D) were measured by ELISA. Total proteins were extracted and the expression of β-catenin (E) and p-AKT (F) were detected by Western blot. The images show the most representative of the three independent experiment performed. To describe cell migration ability, consistently shaped wounds were made during transfection and EPI treatment. Three images were captured at 0, 4, 8 and 22h in the same coordinates. Gap size of the wounds were analyzed using ImageJ software to determine a free-cell

scratch area (G). Micrographs show most representative of three independent experiments (H). N = 3, as mean ± SEM. *p<0.05 **p<0.01 ***p<0.001.

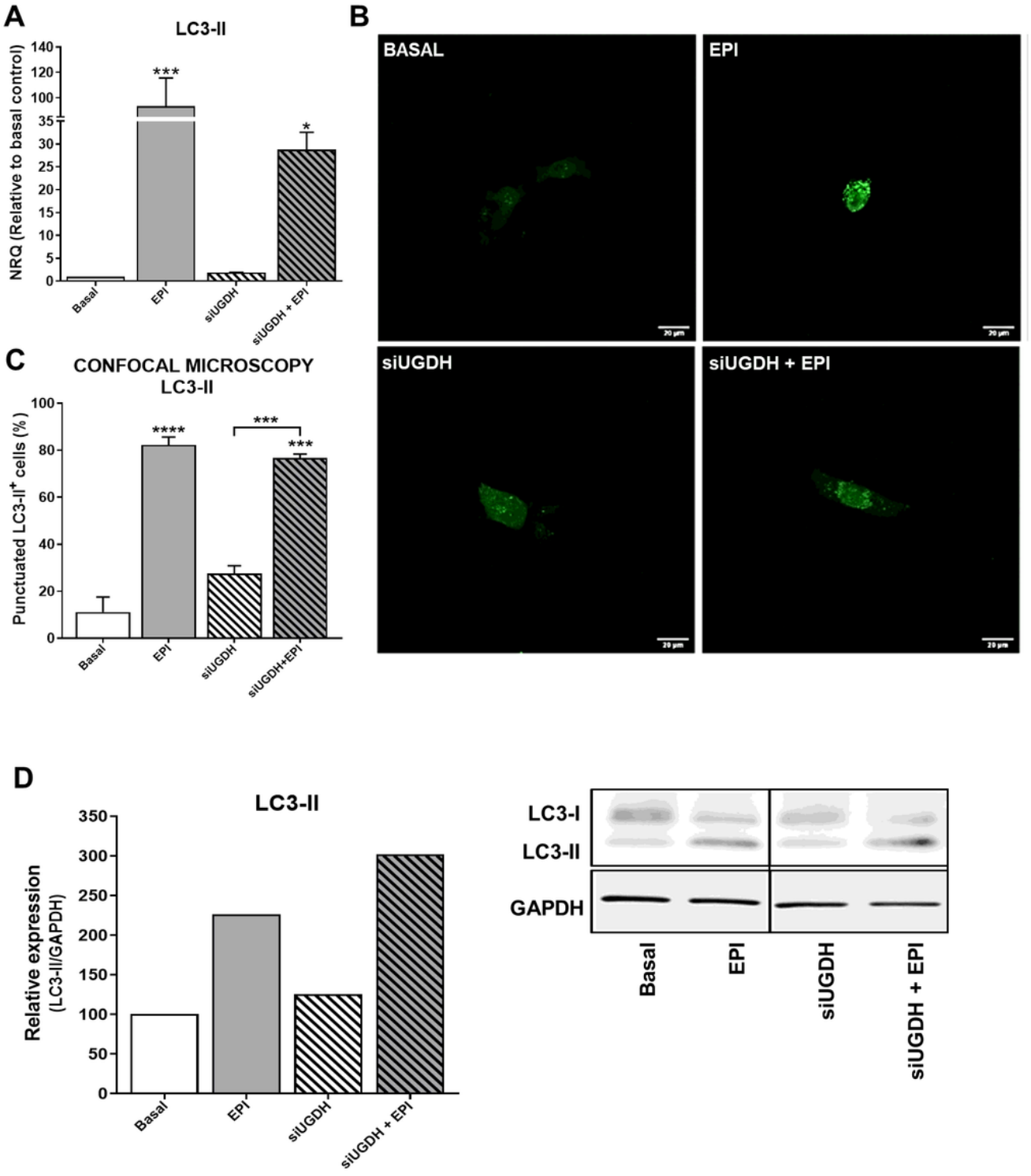

Figure 5

Analysis of autophagy induction as response of knockdown of UGDH enzyme and EPI treatment. MDA-MB-231 cells were co-transfected with a specific siRNA against UGDH gene (siUGDH) or a random sequence siRNA as negative control (siSCR) and 2 ug of a specific LC3-GFP construct. After 24h, 1 μM

EPI (1 EPI) was added to complete 48h of incubation. LC3-II expression (A) was determined by real time quantitative PCR using SYBR Green. Results were normalized using β-actin as reference gene and all determinations were performed as duplicates. To analyze the formation of autophagosomes, the fluorescence emitted by GFP was evaluated through confocal microscopy (B). The LC3-II puncta analysis was performed using the ImageJ software (C). Transformation of LC3-I in LC3-II was evaluated by Western blot, comparing both with GAPDH reference protein (5D). N=3, as mean ± SEM *p<0.05 *** p<0.001.

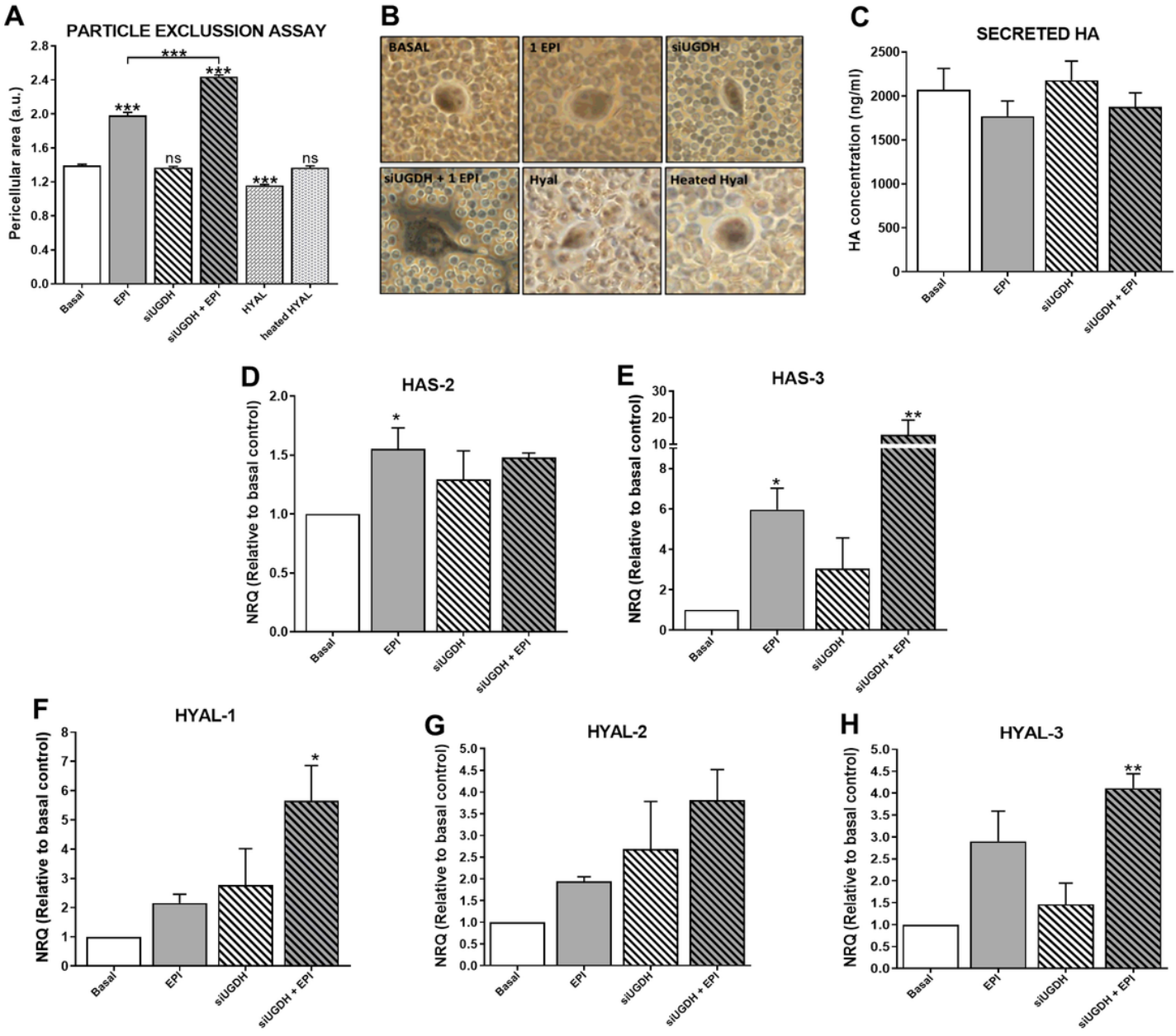

Figure 6

Evaluation of ECM variations as consequence of silencing of UGDH and EPI treatment. MDA-MB-231 cells were transfected with a specific siRNA against UGDH gene (siUGDH) using a random sequence siRNA as negative control (siSCR). After 24h, 1 μM EPI (1 EPI) was added to complete 48h of incubation.

To perform the particle exclusion assay, 2 x 107 fixed red blood cells were added to each well. After allowing to decant, multiple images were captured and analyzed using ImageJ software (A). Micrographs show most representative of three independent experiments (B). Secreted HA in cell supernatants were measured by ELISA (C). HAS2 (D), HAS3 (E), HYAL-1 (F), HYAL-2 (G) and HYAL-3 (H) expression were obtained by real time quantitative PCR using SYBR Green or Taqman probes. Results were normalized using β-actin as reference gene and all determinations were performed as duplicates. N=3, as mean ± SEM *p<0.05 **p<0.01 *** p<0.001.

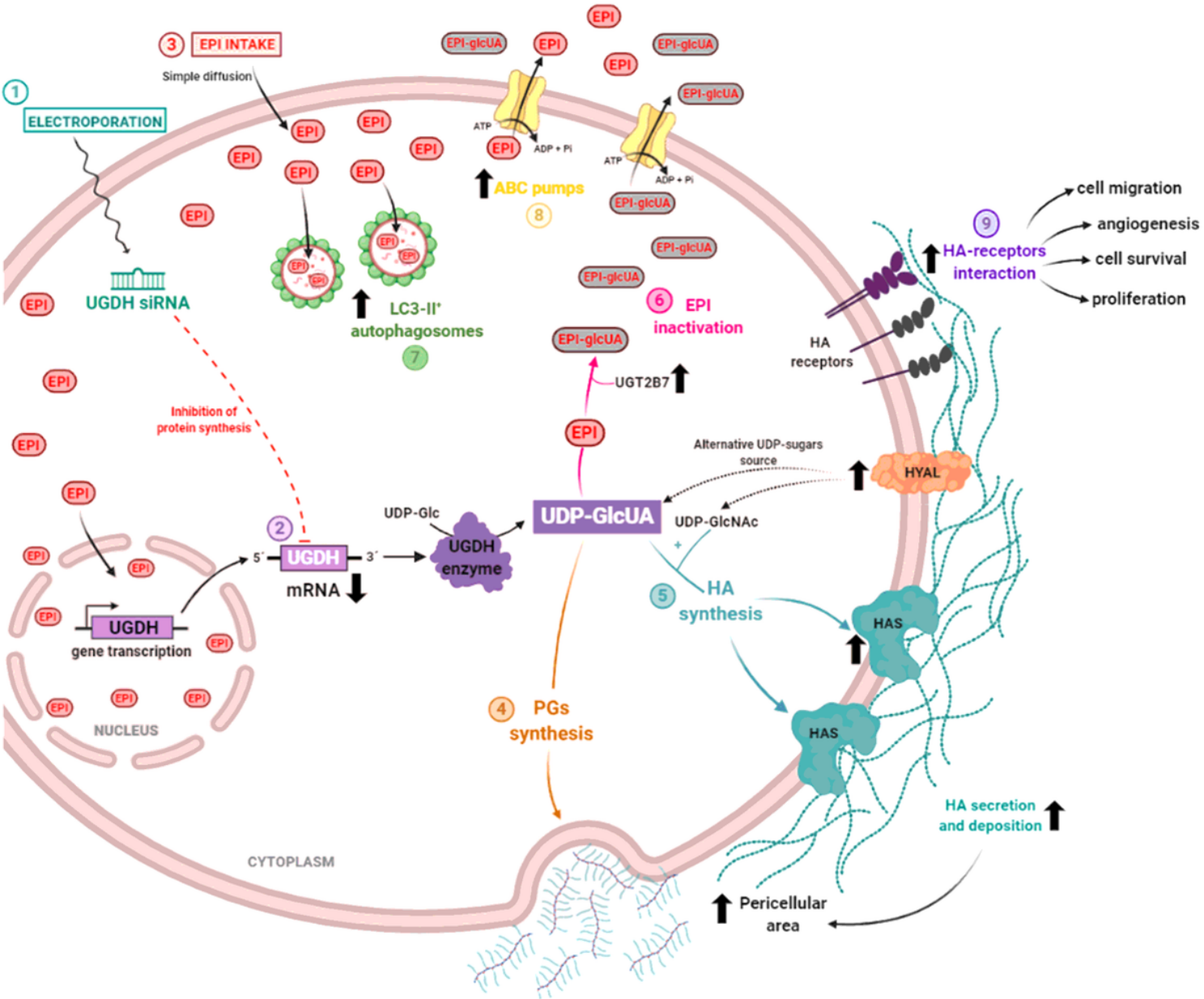

Figure 7

Proposed mechanism of epirubicin resistance in breast cancer cells during UGDH knockdown. MDA-MB-231 cells were transfected to introduce the siRNA against UGDH mRNA (1). UGDH translation and synthesis was blocked due to the specific binding of UGDH siRNA to mRNA. UGDH enzyme is responsible

for the transformation of UDP-glucose (UDP-Glc) into UDP-glucuronic acid (UDP-GlcUA) (2). Twenty-four hours after transfection, tumor cells were treated with epirubicin (EPI). EPI goes across the cell membrane thanks to its hydrophobic structure. An increase in the intracellular accumulation of EPI was observed, being able to be found both in the cytoplasm and in the nucleus (3). UDP-GlcUA is a precursor for different cellular processes involved in extracellular matrix and EPI resistance. Specifically, it can be a constituent of different proteoglycans (PGs) and glycosaminoglycans (GAGs), which contributed to the increase of pericellular area of tumor cells (4). In combination with UDP-GlcNAc, by action of hyaluronan syntheses (HASes), UDP-GlcUA is a precursor of the glycosaminoglycan hyaluronan (HA). Unexpectedly, HAS expression and HA synthesis increased after EPI treatment and UGDH knockdown, which also contributed to the increase in the pericellular area (5). Another interesting mechanism observed was the increase in the expression of HA-degrading enzymes (HYALs). It has been proposed as a new source of UDP-sugars to compensate for the decrease in UGDH enzyme, and therefore UDP-GlcUA availability. Third mechanism in which UDP-GlcUA is involved is the inactivation of EPI. Due to the action of the UGT2B7 transferase, UDP-GlcUA binds to EPI to inactivate its molecule and diminishes EPI activity in tumor cells. During UGDH knockdown, EPI treatment increased UGT2B7 expression favoring EPI inactivation (6). Within the mechanisms activated to avoid EPI activity, an increase in autophagy was detected; process previously shown to be involved in the development of EPI resistance (7). In agreement, it was observed the up-regulation of drug efflux pumps (ABC family) in response to EPI treatment (8). Finally, we hypothesized that an increase in the expression and deposition of HA positively contribute to develop a resistant phenotype by tumor cells. This may be due to an increase in the interaction between HA and its specific receptors, which might be promoting mechanisms involved in tumor progression, such as angiogenesis, migration, cell survival and proliferation, demonstrated during the present study (9).